Internship report

Method comparison of Fourier Transformation infrared spectroscopy (FTIR), optical-photothermal infrared spectroscopy (O-PTIR) and photo-induced force microscopy (PiFM) using various retina and PMMA samples

Written by

Robin Schneider

Supervisor

Dr. Daniela Täuber

Department Microscopy

Leibniz Institute for Photonic Technologies

Contents

1 Theoretical aspects of vibrational spectroscopy

Infrared (IR) -absorption occurs when the energy of incident IR-light with general wavelengths between 800 nm and 1 mm (E = hν) matches the energy difference ΔE between two vibrational states of a molecule (Baker et al. 2016). These energy differences ΔE are chemically characteristic for each covalent chemical bond in a molecule, such that every IR-active molecule provides a characteristic IR-absorption spectrum. But in general, only molecules with a changeable or inducible dipole moment are IR-active. Further the excitation by IR-light induces various phenomena in the samples, like thermal expansion or a change in the molecular electromagnetic dipole.

1.1 Fourier Transformation IR spectroscopy (FTIR)

The most established form of infrared spectroscopy is the Fourier Transformation infrared spectroscopy (FTIR). The Fourier Transformation is used for enhancement of the signal-to-noise ratio because typically IR-absorption spectra are weak. The lateral resolution of FTIR is mainly diffraction limited by the wavelength of the incident IR-light (for mid-IR: 2,5 - 25 µm).

1.2 Optical-photothermal infrared spectroscopy (O-PTIR)

The optical-photothermal IR spectroscopy (O-PTIR) uses a visible (VIS) or near-IR (NIR) probe to detect the photothermal IR-effect. O-PTIR operates with high speed, pulsed and tunable IR lasers, which are focused onto the sample surface (Fig. 1). When the incident IR laser is tuned to a wavelength, that induces IR absorption, the excited regions of the sample rapidly heat up and the photothermal response is measured via a visible laser beam, focused to a much smaller spot than the IR beam (Photothermal Spectroscopy Corporation 2020). Thereby O-PTIR provides a better lateral resolution than FTIR due to the VIS or NIR beam wavelength of the detection laser and in this way IR spectroscopy and chemical imaging are independent of IR wavelength. Such that it is possible to get lateral resolutions between 0,5 and 1 µm. Moreover, even if O-PTIR measures in reflection mode the absorption spectra show FTIR transmission-like quality (Photothermal Spectroscopy Corporation 2020).

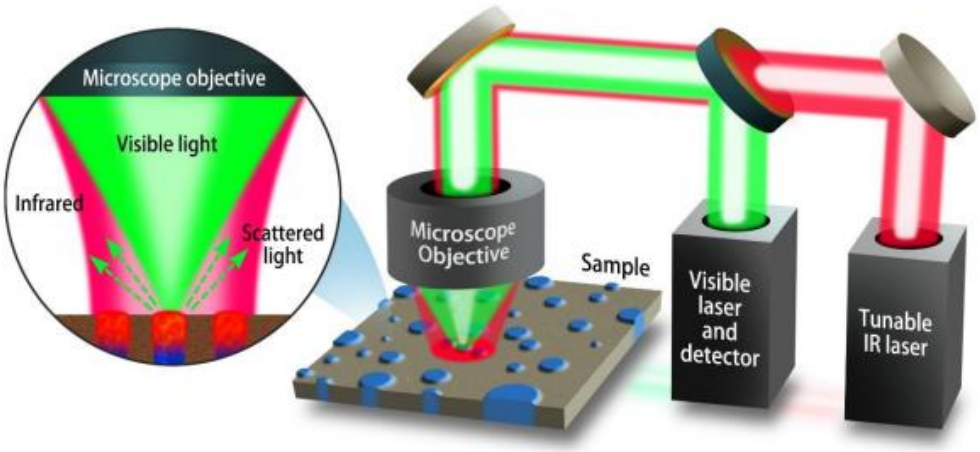

Figure 1: O-PTIR setup (Photothermal Spectroscopy Corporation 2020)

1.3 Photo-induced force microscopy (PiFM)

Photo-induced force microscopy (PiFM) is based on atomic force microscopy (AFM), in which the sample surface is mechanically scanned with a sharp tip and atomic forces between the tip and the sample bend the cantilever, on which the tip is mounted. The interaction force F_{ts} between tip and sample depends on the tip-sample distance z and the spring constant of the cantilever. Examples for these acting forces are Van der Waals-, capillary-, electrostatic- or magnetic dipole-forces and chemical bonding. For signal detection the bending of the cantilever is measured, whereby conclusions to the acting force between sample atoms and tip can be drawn.

For PiFM comes in addition that the sample molecules are excited with IR-light. For this mostly mid-IR (MIR) light is used. MIR light interacts with sample molecules in various ways. On the one hand it induces a change in electromagnetic dipole μ_s and on the other hand it induces, on thermal expansion based, interaction forces (e.g., effective Van der Waals forces), but the exact composition of this interaction force is still a current research subject. PiFM also uses mechanical detection of the interaction force, which is mostly measured in an attractive regime, between the sample and a metallic AFM-tip. In general, this in z-direction acting force is in a range of a few pN, what enables a high lateral resolution below 10 nm (Li et al. 2020). For so called heterodyne detection in dynamic AFM-mode, in which the cantilever is driven at its second mechanical resonance f_1 and the detection of PiFM signal is carried out at the first mechanical resonance f_0. Further the incident light of tunable quantum cascade lasers (Fig. 2) is polarized along the tip axis and pulsed at the frequency $f_m = f_1 - f_0$ (Le Wang et al. 2019).

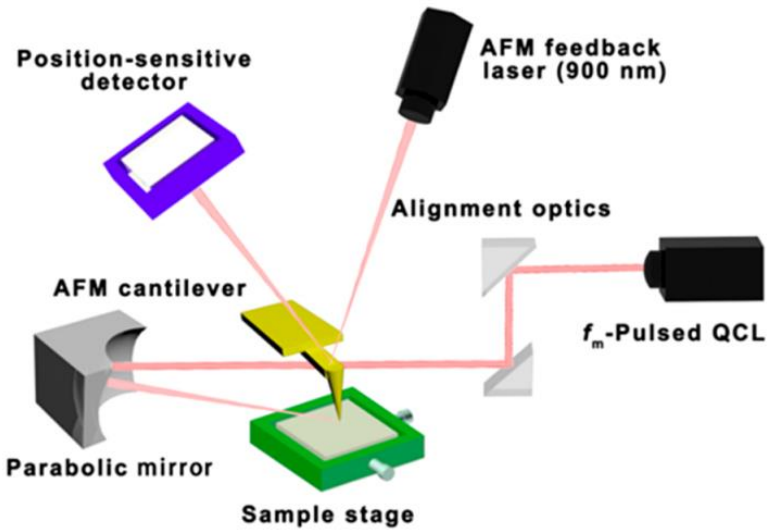

Figure 2: PiFM setup (Li et al. 2020)

2 Material and methods

2.1 Samples and sample preparation

Polymethyl methacrylate (PMMA) is a transparent thermoplastic, also known as acrylic glass or plexiglass. The investigated samples were PMMA films of a photoresist of varied thicknesses (60 - 2000 nm) on three substrates. First on sputtered gold (Au) substrates consisting of 50 nm Au on top of 3 nm titanium (Ti) onto polished silicon. More samples were prepared directly on silicon or CaF_2. All PMMA samples were provided by Uwe Hübner (Competence Center for Micro and Nanotechnologies, Leibniz-IPHT, Jena).

Further four substances of human retina were analyzed. First there is all-trans retinal, a carotenoid, the aldehyde of retinol, also known as Vitamin A1. Retinyl palmitate, the ester of retinol and palmitic acid, which is mostly used for vitamin A storage, was the second sample. Moreover melanin, a natural pigment found in most organisms and an effective absorbent of UV and VIS-light and L-α-phosphatidylcholine, a phospholipid and major component of herbal and animal membranes, were used. All these retina samples were first solved in an appropriate solvent. For all-trans retinal and retinyl palmitate methanol, for melanin dimethyl sulfoxide (DMSO) and for L-α-phosphatidylcholine chloroform, was used. Afterwards the sample solutions were dripped onto CaF_2 substrates and air dried at room temperature before the measurements.

2.2 FTIR measurements

The FTIR measurements were done using a VARIAN 620-IR FT-IR Imaging Microscope with a liquid nitrogen cooled mercury cadmium telluride (MCT) detector with a resolution of 2 cm^{-1}, a spectral range of 750 to 4000 cm^{-1} and 8 scans for each sample absorption spectrum. The angle of incidence of IR-light is 0° and the aperture was set at 100 x 100 µm. All retina samples, PMMA films on silicon and on CaF_2 were measured in transmission mode. The PMMA films on Au and additionally also the PMMA samples on silicon were measured in reflection mode.

2.3 O-PTIR measurements

For O-PTIR measurements a mIRage™ system from Photothermal Spectroscopy Corporation (Santa Barbara, CA) integrated with a four-module pulsed quantum cascade laser (QCL) system, with a tunable range of 790 to 1806 cm^{-1}, a resolution of 2 cm^{-1} and 2 scans for each sample spectrum, was used. The NIR detection laser was set at 785 nm and the angle of incidence of NIR and MIR-light is 0°. All samples were measured in reflection mode on a reflecting metal coated substrate.

2.4 PiFM measurements

A VistaScope from Molecular Vista integrated with a four-module pulsed quantum cascade laser (QCL) system, with a tunable range of 770 to 1890 cm^{-1} and a wavenumber resolution of 1 cm^{-1} was used. As already mentioned, the signal detection is done in dynamic mode, the, so called heterodyne detection, with NCH-Pt 300 kHz noncontact cantilevers (type PPP-NCHPtx64-MB-10) from Nanosensors. Consequently, the cantilever was driven at its second harmonic resonance ($f_1 \approx 1750$ kHz), and the photo-induced force was detected at the first harmonic resonance ($f_0 \approx 280$ kHz). The pulses of the four tunable quantum cascade lasers (QCLs) were modulated at the difference $f_m = f_1 - f_0$ with 40 ns pulse duration. The angle of incidence of IR-light is 80° and the light of the four QCLs is co-aligned and linearly polarized in the plane of incidence (p-polarization). Spectra were acquired over 100 s with IR-light intensity clipped at 1% of the maximum intensity previously recorded in the power spectrum.

2.5 Data evaluation

Data pre-processing and spectra selection were done with PTIRStudio v.4.3 for O-PTIR and SurfaceWorks 2.4 Release 22 and 23 for PiFM measurements. Background correction for FTIR spectra was carried out with an in-house python program provided by Mohammad Soltaninezhad. All spectra were averaged, scaled, and displayed with SciDAVis. Vector normalization was done with Microsoft Excel.

3 Results and discussion

3.1 PMMA samples on Au

All PMMA photoresist films with thicknesses between 60 and 2000 nm on Au substrates measured with FTIR in reflection mode show three important spectral regions (Fig. 3). Between 1750 and 1700 cm^{-1} there is the C=O ester bond stretching located and between 1500 and 1375 cm^{-1} there are the C-H methyl group bending's. Both, C-O ester, and ether bond stretching's are to be found in the spectral region of 1300 to 1100 cm^{-1}. Other low intensity peaks at lower wavenumbers probably belong to C-H bending vibrations. Even if the thinnest sample (60 nm) is displayed with tenfold intensity this shows still the lowest intensity for all absorption bands. For increasing PMMA thicknesses an also increasing FTIR signal intensity is observed, as expected. Further the intensity ratios between the C=O stretching region and all other vibrations change within the 2000 nm PMMA sample and the peak position for the 1730 cm^{-1} peak is shifted to higher wavenumbers, like for the 60 nm sample (Fig. 3). Shifting peak positions over various PMMA film thicknesses on Au of the C=O stretching vibration compared to C-O ester and C-H methyl vibrations are shown in the attachment (Fig. A1 - A3).

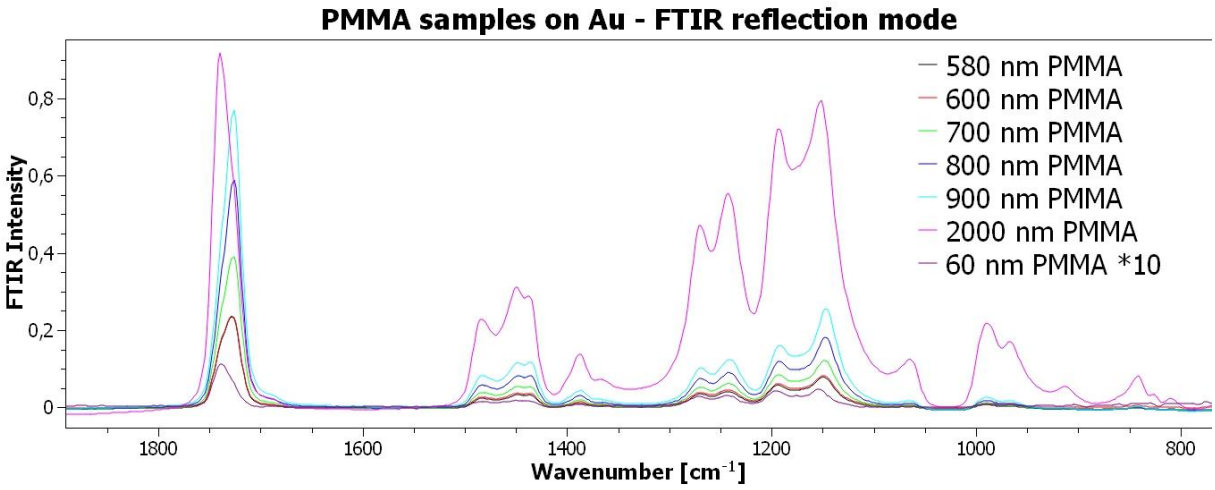

Figure 3: PMMA photoresist films with various thicknesses on Au substrates measured with FTIR in reflection mode.

For comparative O-PTIR measurements it is firstly required to choose a suitable IR-laser intensity for excitation, that avoids damaging the sample. Because otherwise the detected O-PTIR intensity could decrease, and chemical melting processes probably could be observed. This is demonstrated in figure 4, in which the 700 nm PMMA sample on Au is measured with various IR-laser intensities and probe powers. It can be noticed, that the O-PTIR signal intensity is clearly decreasing if the same spot is measured shortly after with 59% IR-laser intensity and 37% probe power (Fig. 4 A). Moreover, the third measurement already shows changes in the absorption spectrum, for example at the 1750 - 1700 cm^{-1} spectral region. The problem with the decreasing O-PTIR signal, while measuring a randomly chosen spot, is likewise observed if only the probe power is reduced to 20% (Fig. 4 B) or additionally the IR-laser intensity is reduced to 47% (Fig. 4 C).

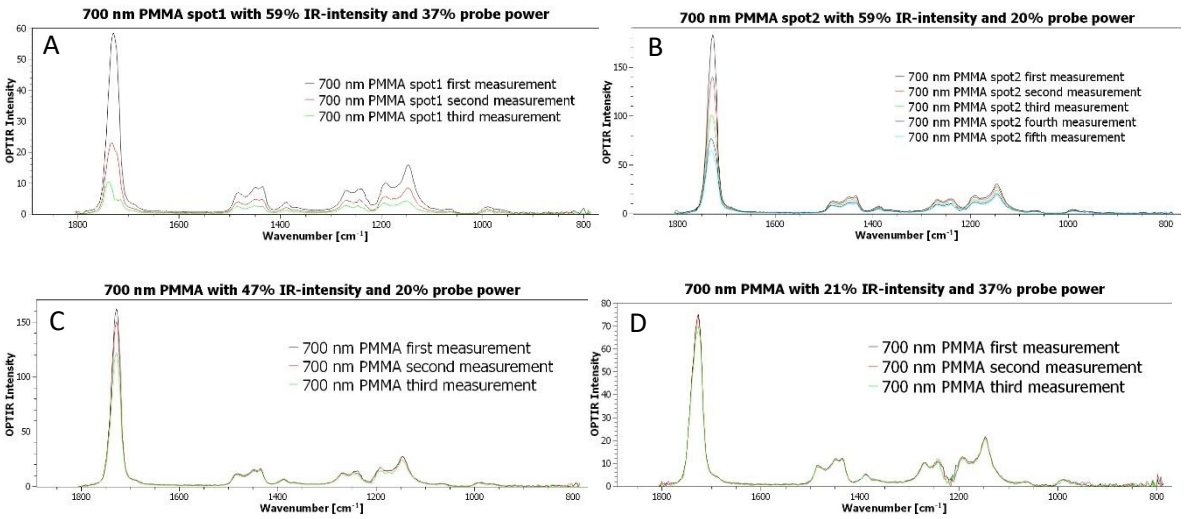

*Figure 4: 700 nm PMMA sample measured with various IR-laser intensities (O-PTIR). (**A**) three consecutive measurements at the same spot (spot1) with 59% IR-laser intensity and 37% probe power. (**B**) five consecutive measurements at another spot (spot2) on the same sample with 59% IR-laser intensity and 20% probe power. (**C**) three consecutive measurements at a third spot (spot3) with 47% IR-laser intensity and 20% probe power. (**D**) three consecutive measurements with 21% IR-laser intensity and 37% probe power at spot4.*

A further reduced IR-laser intensity to 21% leads to a more stable signal intensity within three consecutive measurements at a spot (Fig. 4 D). Thus, the following measurements of 60 – 2000 nm PMMA films were carried out with 21% IR-laser intensity. Moreover, 37% probe power was used to increase the overall O-PTIR intensities. This is justified by the generally lower signal intensities with lower IR-laser intensities and the influence of the probe power on damaging the samples to be rather low.

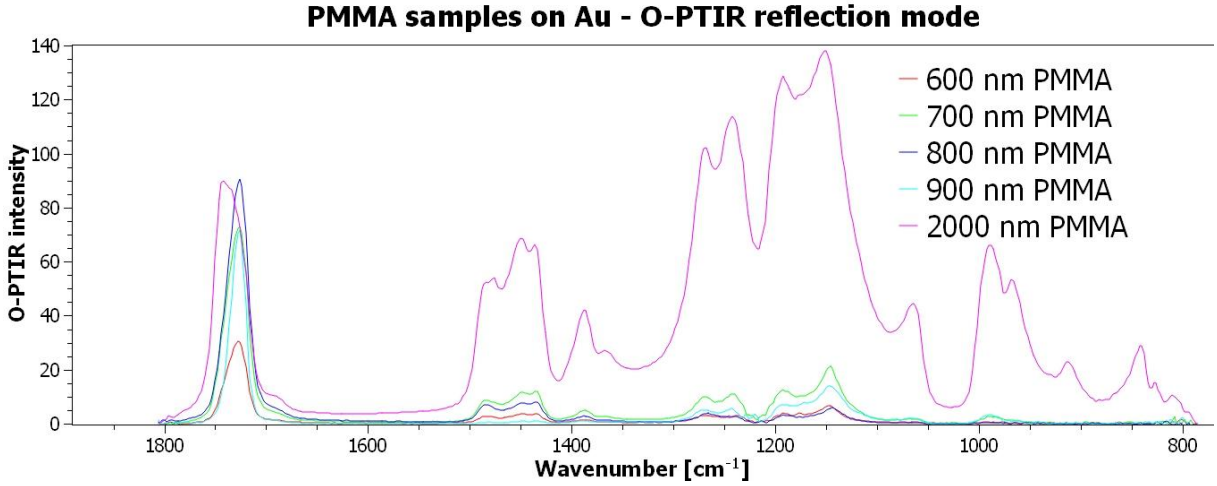

Figure 5: PMMA photoresist films with various thicknesses on Au substrates measured with O-PTIR (21% IR-laser intensity and 37% probe power), without 60 nm sample due to an indiscernible peak structure in the absorption spectrum.

The O-PTIR results for the PMMA samples on Au demonstrate no clear intensity distribution, as observed for FTIR absorption spectra. For example, shows the 800 nm sample a higher intensity at the spectral region of 1500 to 1425 cm^{-1} than at wavenumbers between 1300 and 1100, during the intensity distribution for the 900 nm sample is the other way around. But again, the intensity ratios

between the C=O stretching region and all other vibrations change within the 2000 nm PMMA sample and the peak position for the 1730 cm^{-1} peak is shifted to higher wavenumbers (Fig. 5, A1 -A3). One possible cause could be, that there are interferences by reflection at interfaces like at the Au-PMMA-interface. Continuing the change of the refractive index due to photothermal expansion could be a reason or additional interference effects of the probing NIR-laser for O-PTIR and polarization of light might play a role, too. The 60 nm PMMA sample delivered no signal in the absorption spectrum due to the issue that suitable samples for O-PTIR should be thicker than 200 nm (Photothermal Spectroscopy Corporation 2020).

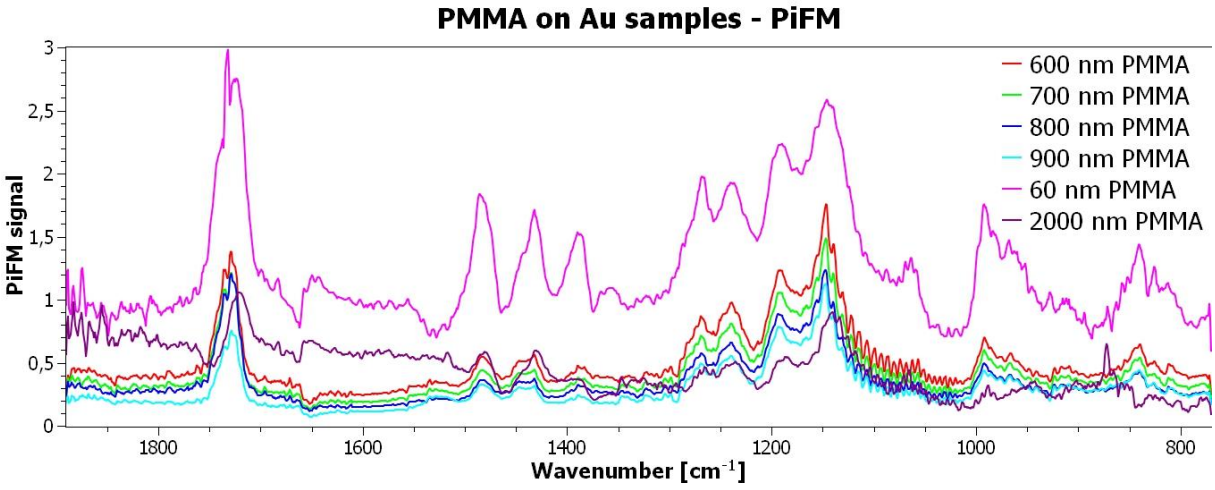

Figure 6: PMMA photoresist films with various thicknesses on Au substrates measured with PiFM. All spectra are averaged, scaled and smoothed (Savitzky-Golay with a polynominal degree of 2 over 2x3 points).

The PMMA photoresist films with thicknesses between 60 and 2000 nm on Au substrates measured with PiFM show a decreasing signal intensity with increasing film thicknesses at the spectral region between 1300 and 1100 cm^{-1} (Fig. 6). A possible cause to this aim could be, the angle of incidence of IR-laser light, which is 80° for PiFM and 0° for FTIR and O-PTIR. For the remaining spectral regions, this correlation is likewise correct for the PMMA films between 60 and 900 nm, except for the 2000 nm sample, in which an irregular peak at 940 cm^{-1} and a possibly higher background at wavenumbers higher than 1300, is observed. A reason therefore could be that the 2000 nm sample was measured with a different tip (same type) and on another measurement day. Moreover, a various peak structure at 1450 – 1375 cm^{-1}, compared to the FTIR and O-PTIR measurements, can be observed. Another observation are the fringes in the spectral region of 1150 to 1050 cm^{-1} with the 600 – 900 nm films, which are not visible in the 60 and 2000 nm samples. This might come from a cavity-effect between the bottom of the cantilever and one or even more reflecting surfaces of the PMMA films, for example the gold or silicon surfaces. Further, the intensity ratios between the 1730 cm^{-1} peak and the remaining spectral features, in contrast to the FTIR and O-PTIR results, seems to be comparable for all samples (Fig. 6).

3.2 PMMA samples on Si

The PMMA photoresist films with various thicknesses between 1000 and 2000 nm on Si substrates measured with FTIR show the same spectral features, like the PMMA samples on Au (Fig. 7 and 8). In line with the FTIR results of PMMA on Au and the angle of incident IR-light of 0°, an increasing intensity with increasing film thicknesses is observed for measurements in transmission (Fig. 7).

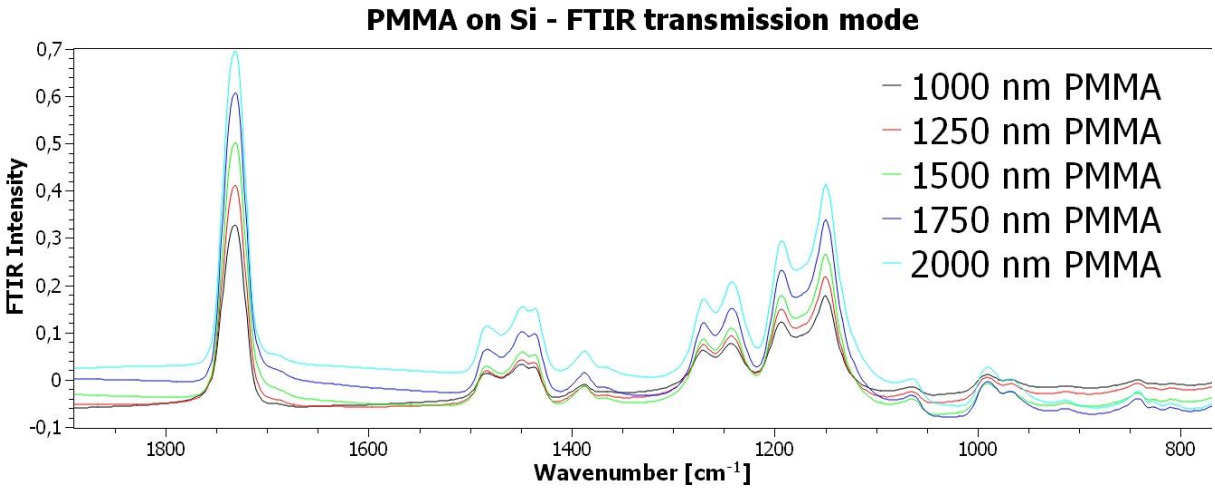

Figure 7: PMMA photoresist films with various thicknesses on Si substrates measured with FTIR in transmission mode.

In general, the PMMA films on Si measured in reflection mode FTIR, likewise show an increasing signal intensity with increasing film thicknesses (Fig. 8). But there also is some interference effect visible in the absorption spectra. Possible causes to this aim could be a combination of the so-called electric field standing wave (EFSW) effect and other interferences, yielding various band intensity ratios and band positions depending on the thickness of the sample (Mayerhöfer et al. 2018). In addition to the EFSW effect, there is one more possible interference effect, which is caused by dispersion and can lead to asymmetric band shapes (Mayerhöfer et al. 2018).

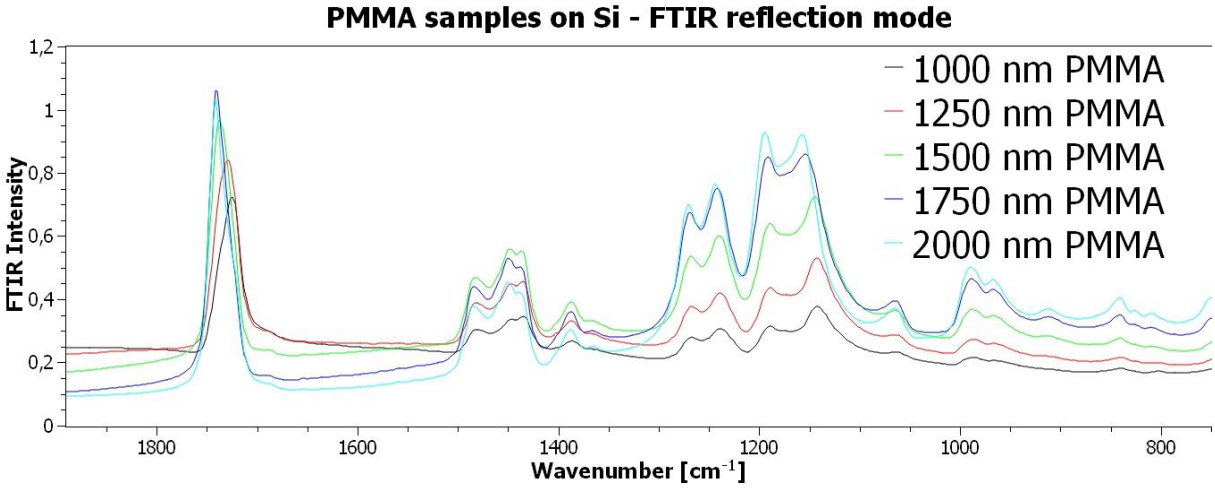

Figure 8: PMMA photoresist films with various thicknesses on Si substrates measured with FTIR in reflection mode.

A decreasing signal intensity with increasing PMMA photoresist film thicknesses is observed, on Si substrates measured with PiFM (Fig. 9). This effect was likewise visible in the PMMA sample spectra on Au (Fig. 6) and is related to the 80° angle of incidence of IR-laser light during PiFM measurements. Compared to the PiFM results on Au the spectral regions in the absorption spectra of the PMMA samples on Si are similar, apart from the C-H methyl vibrations (1500 – 1375 cm^{-1}). These show here no three clearly separated peaks. Indeed, there can be observed two features with a fine structure in the same spectral region (Fig. 9).

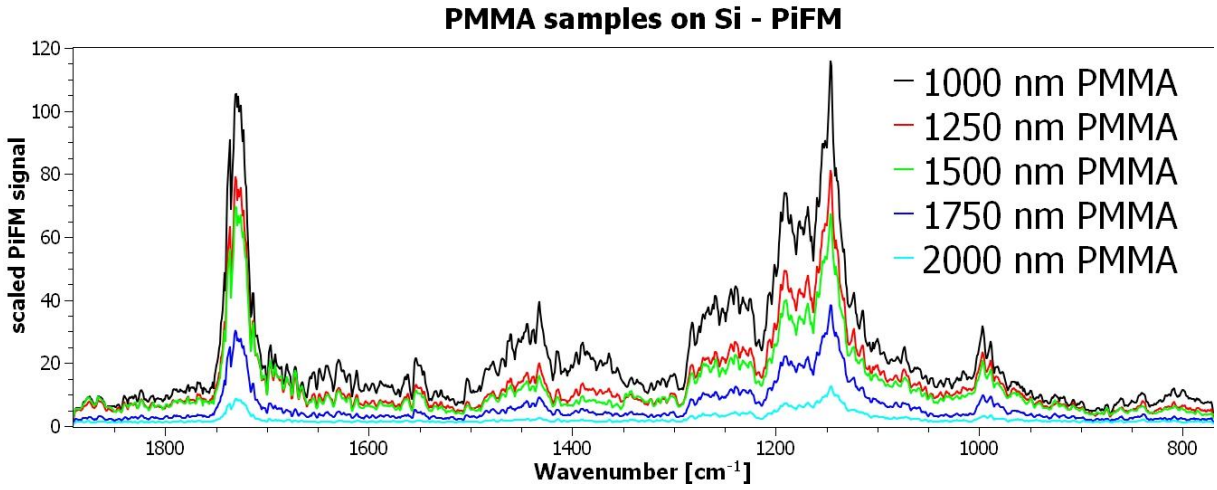

Figure 9: PMMA photoresist films with various thicknesses on Si substrates measured with PiFM. All spectra are averaged, scaled, and smoothed (Savitzky-Golay with a polynominal degree of 2 over 2x3 points)

3.3 PMMA samples on CaF_2

The PMMA photoresist films with various thicknesses between 1000 and 2000 nm on CaF_2 substrates measured with FTIR in transmission mode, again, show the same spectral features, like the PMMA samples on Au and on Si. In line with these previous FTIR results and the angle of incident IR-light of 0°, an increasing intensity with increasing film thicknesses is observed (Fig. 10).

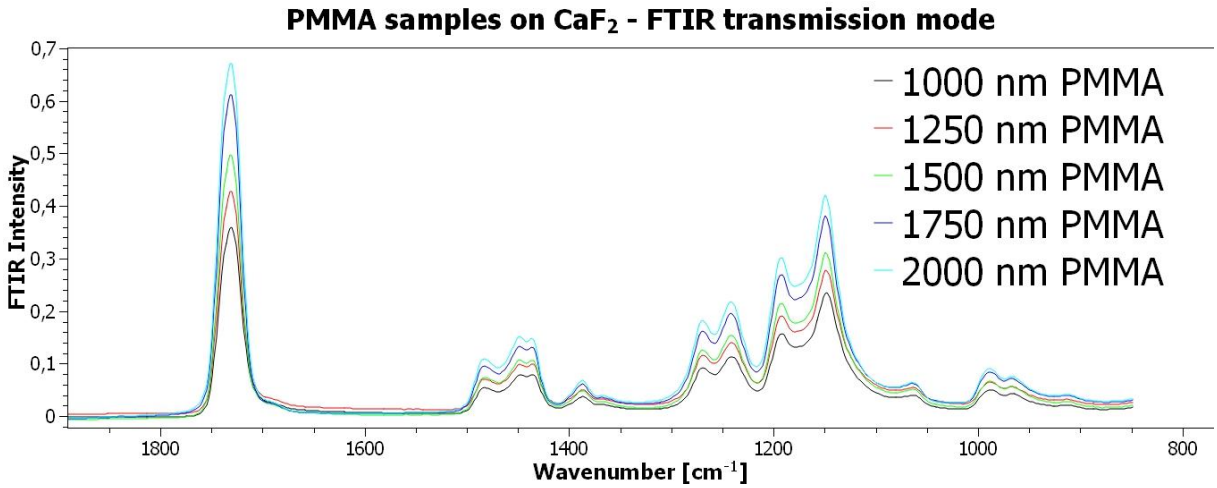

Figure 10: PMMA photoresist films with various thicknesses on CaF_2 substrates measured with FTIR in transmission mode.

No correlation between signal intensity and thickness is observed for the PMMA films with various thicknesses on CaF_2 substrates measured with PiFM (Fig. 11). It must be noted, that the 1000 nm and 2000 nm PMMA samples were recorded with a different tip of the same type, compared to the remaining samples (1250 – 1750 nm). But even the measurements with the same tip does not show a correlation between signal intensity and thickness. Generally, the PiFM spectra are similar with all three substrates (Au, Si and CaF_2) and the same spectral regions exhibit signals. The peak structure for the C-H methyl vibrations (1500 – 1375 cm^{-1}) shows different features, compared to PMMA films on Au, but is more like the samples on Si. But in comparison to the PMMA samples on Si and on CaF_2 there is no comparable fine structure observed over the whole spectrum (Fig. 9 and 11). Overall, the interpretation of PiFM results of PMMA films on Si and CaF_2 should be handled carefully due to occurring signal dips and at times inhomogeneous excitation of the four QCLs.

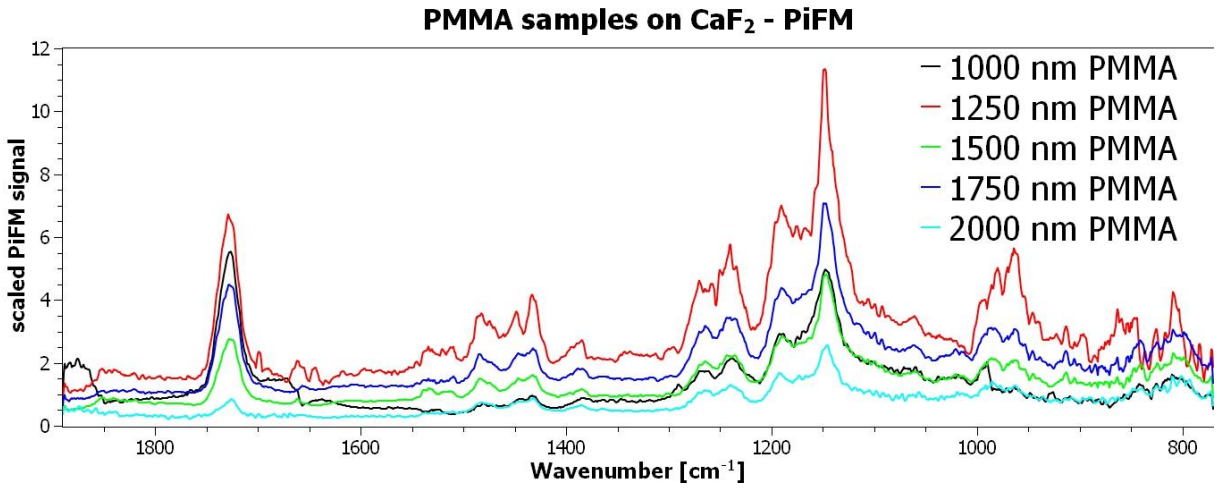

Figure 11: PMMA photoresist films with various thicknesses on CaF_2 substrates measured with PiFM. All spectra are averaged, scaled, and smoothed (Savitzky-Golay with a polynominal degree of 2 over 2x3 points). 1000 nm PMMA and 2000 nm PMMA samples were recorded with a different tip, compared to the remaining samples (1250 – 1750 nm).

3.4 Retina samples

For a further comparison of the three methods FTIR, O-PTIR and PiFM, especially in relation to suitability of various sample types and resolution, four substances of human retina were analyzed. These are all-trans retinal, melanin, retinyl palmitate and L-α-Phosphatidycholine. All displayed figures contain averaged and vector normalized spectra of all methods to be compared. Additionally, the most intense absorption bands for each sample are assigned to their associated vibrations. The results of L-α-Phosphatidycholine show similar absorption spectra for FTIR and O-PTIR, in which the same spectral regions become evident (Fig. 12). But it can be observed that with O-PTIR it is possible to distinguish more features in some spectral regions than with FTIR, like for the C-O alkoxy vibrations between 1100 and 1040 cm^{-1} or the C=O ester vibrations at 1730 cm^{-1}. This might be caused by the higher lateral resolution of O-PTIR (785 nm) compared to FTIR, which delivers rather bulk measurements with a resolution of a few micrometers. Interpretation of the PiFM results should be handled carefully due to occurring signal dips and at times inhomogeneous excitation of the four QCLs. To this aim it is important to know, where the transitions of QCLs are. The first transition is located at ≈1660 cm^{-1}, the second one at ≈1350 cm^{-1} and the last one at ≈990 cm^{-1}. In case of L-α-Phosphatidycholine the first and the third transition are visible in the PiFM spectrum (Fig. 12). But still signals of the same spectral regions like with FTIR and O-PTIR are observed, even if the intensity ratios are completely various. For example, the intensity for C=O ester vibrations at 1730 cm^{-1} is much lower, while C-H alkene vibrations (810 cm^{-1}) show a higher intensity compared to O-PTIR. This, on the one hand could be caused by inhomogeneous excitation of the QCLs and on the other hand by problems to achieve a stable signal with the AFM-tip on greasy substances, like phospholipids to which L-α-Phosphatidycholine belongs.

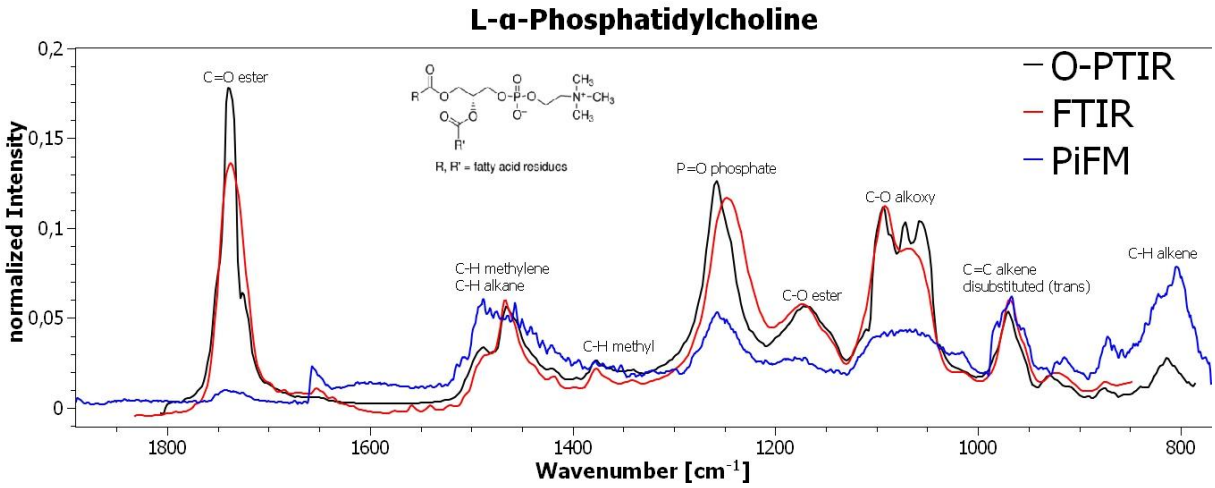

Figure 12: L-alpha-Phosphatidylcholine measured with FTIR, O-PTIR and PiFM in comparison. All spectra are displayed after vector normalization. PiFM spectrum, in addition, is scaled and smoothed (Savitzky-Golay with a polynominal degree of 2 over 2x3 points).

For melanin, the assignment of absorption bands shows that especially in the spectral region between 1730 and 1250 cm^{-1} many vibrations overlay each other, yielding a high background and just a coarse structure with no clearly separated peaks (Fig. 13). Due to the low volatility of the solvent used for melanin, the FTIR spectra and in traces also the O-PTIR spectra include the S=O vibration of DMSO at 1010 cm^{-1} and possibly a signal for C-H methyl vibrations of DMSO (1450 – 1375 cm^{-1}), too. Not displayed in this graphic is the relatively low O-PTIR intensity for melanin compared to the remaining retina samples, which might be caused by the high absorption ability of melanin also at the NIR detection wavelength of O-PTIR. The PiFM results show roughly the same absorption maxima compared to FTIR and O-PTIR, but again two QCL transitions at 1660 and 990 cm^{-1} are visible as sharp edges.

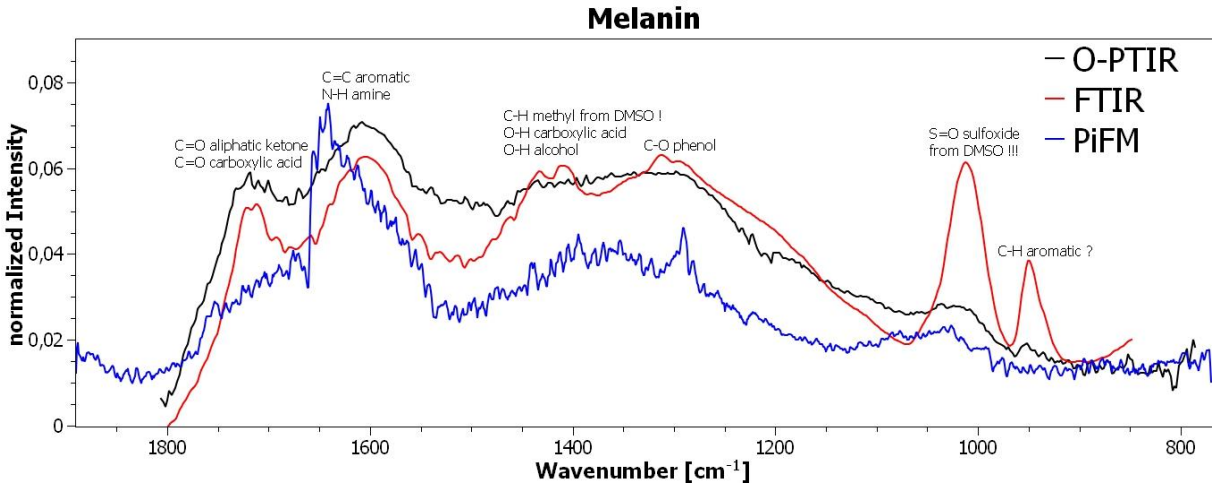

Figure 13: Melanin measured with FTIR, O-PTIR and PiFM in comparison. All spectra are displayed after vector normalization. PiFM spectrum, in addition, is scaled and smoothed (Savitzky-Golay with a polynominal degree of 2 over 2x3 points).

The absorption spectra of retinyl palmitate measured with O-PTIR show some unambiguous differences compared to the FTIR data (Fig. 14). For instance, the C=C alkene vibrations (1580 – 1530 cm^{-1}) are completely missing in the FTIR spectra and C-O alkyl ether vibrations at 1020 cm^{-1} exhibit only a very low FTIR intensity compared to O-PTIR. Further it is possible to distinguish more features in some spectral regions with O-PTIR than with FTIR. For example, the C-H methyl and C-H alkane vibrations between 1400 and 1350 cm^{-1} are better separated with O-PTIR. The only visible structure in the PiFM spectra result of the QCL transitions at 1660 and 1350 cm^{-1} which again result in sharp edges. The missing absorption bands outlines again the problems during measurements to achieve a stable signal with the AFM-tip on greasy and soft samples.

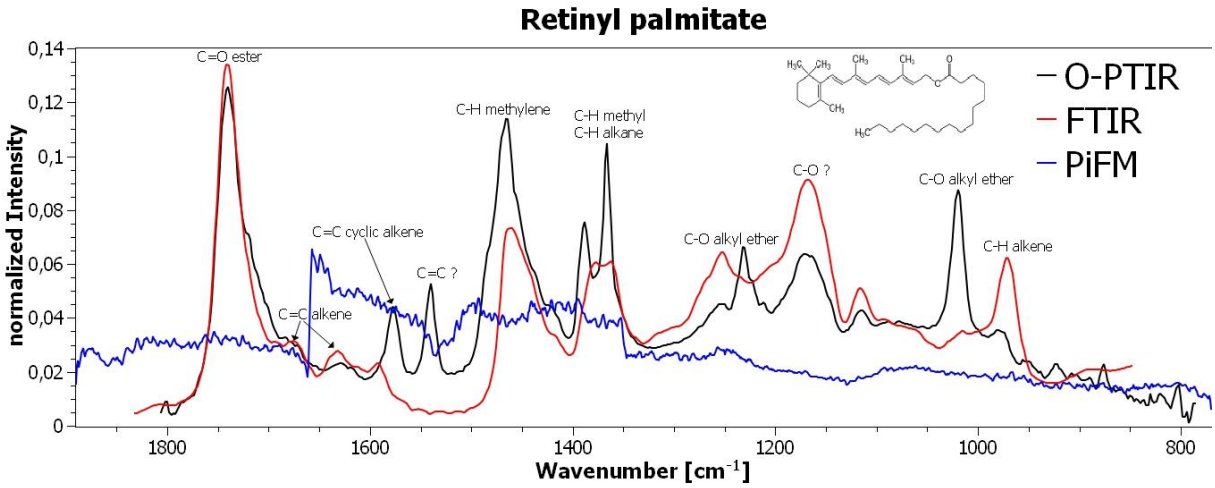

Figure 14: Retinyl palmitate measured with FTIR, O-PTIR and PiFM in comparison. All spectra are displayed after vector normalization. PiFM spectrum, in addition, is scaled and smoothed (Savitzky-Golay with a polynominal degree of 2 over 2x3 points).

All-trans retinal measured with FTIR shows some differences, especially in the spectral region of 1800 to 1550 cm^{-1} compared to the O-PTIR data. O-PTIR points out just one high intense peak with one stronger maximum for the C=O aldehyde vibration (1730 cm^{-1}), a less intense maximum for the C=C alkene vibrations (1670 cm^{-1}) and a shoulder at lower wavenumbers, which might come from C=C cyclic alkene vibrations. With FTIR all these vibrations are clearly separated (Fig. 15). The spectral regions at lower wavenumbers are similar for FTIR and O-PTIR even if O-PTIR seems to contain a generally higher background due to overlapping signals. In the PiFM spectra two sharp edges at 1660 and 990 cm^{-1} are observed, which are caused by the QCL transitions. Further, there is some kind of absorption band structure visible, but which is probably mainly caused by inhomogeneous excitation of the QCLs and their transitions.

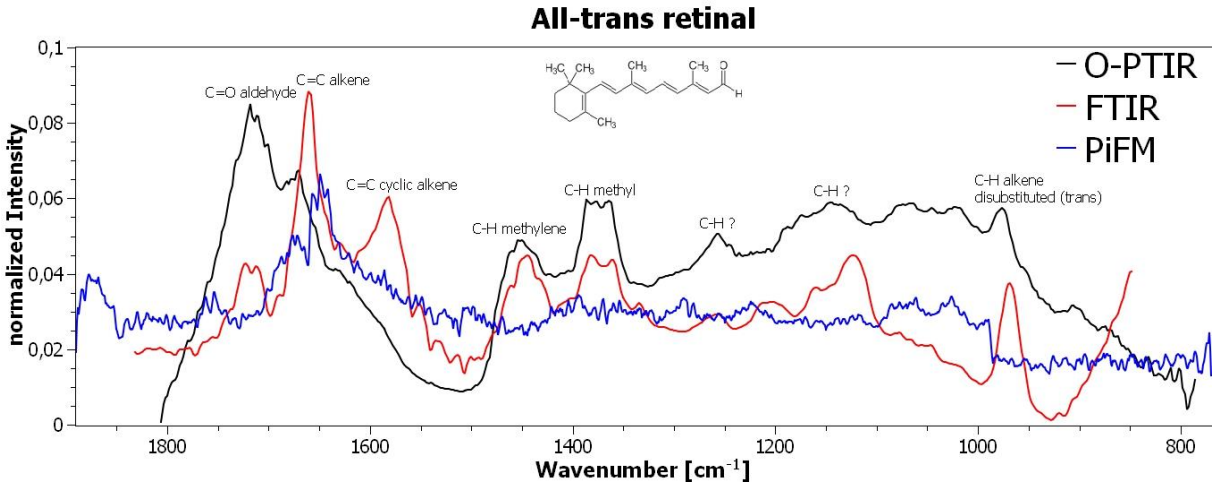

Figure 15: All-trans retinal measured with FTIR, O-PTIR and PiFM in comparison. All spectra are displayed after vector normalization. PiFM spectrum, in addition, is scaled and smoothed (Savitzky-Golay with a polynominal degree of 2 over 2x3 points).

4 Summary

In general O-PTIR enables to resolve more spectral features than FTIR due to its better lateral resolution, like for L-α-Phosphatidylcholine and retinyl palmitate. But for other samples, interferences with the NIR detection probe might limit its spectral feature separation ability. Even the change of the refractive index due to photothermal expansion could be a reason or polarization of light might play a role, too. In line with this correlation PiFM, with its sub 10 nm^2 spatial resolution, should separate the most spectral features, but during the measurements carried out problems with inhomogeneous excitation of the QCLs and their transitions yielding sharp edges and rather random intensity ratios. Additionally, PiFM seems to be rather unsuitable for soft and greasy substances due to problems with achieving a stable signal with the AFM-tip. Moreover, it is important to choose a suitable IR-laser intensity for excitation, that avoids damaging the sample for comparative O-PTIR measurements. Because otherwise the detected O-PTIR signal intensity could decrease, and chemical melting processes probably could be observed. Further, for O-PTIR it should be noted that there might be interferences by reflection at interfaces like at the Au-PMMA-interface of the PMMA samples on Au. This for example can result in an indistinguishable correlation between PMMA film thickness and signal intensity, as observed for O-PTIR absorption spectra for PMMA samples compared to FTIR and PiFM data.

5 List of figures

Bibliography

Baker, Matthew; Hughes, Caryn; Hollywood, Katherine (2016): Biophotonics: Vibrational Spectroscopic Diagnostics. 1. Aufl. Bristol: IOP Concise Physics - A Morgan & Claypool Publication.

Le Wang; Jakob, Devon S.; Wang, Haomin; Apostolos, Alexis; Pires, Marcos M.; Xu, Xiaoji G. (2019): Generalized Heterodyne Configurations for Photoinduced Force Microscopy. In: *Analytical chemistry* 91 (20), S. 13251–13259.

Li, Jian; Jahng, Junghoon; Pang, Jie; Morrison, William; Li, Jin; Lee, Eun Seong et al. (2020): Tip-Enhanced Infrared Imaging with Sub-10 nm Resolution and Hypersensitivity. In: *The Journal of Physical Chemistry Letters* 11 (5), S. 1697–1701.

Mayerhöfer, Thomas G.; Pahlow, Susanne; Hübner, Uwe; Popp, Jürgen (2018): Removing interference-based effects from the infrared transflectance spectra of thin films on metallic substrates: a fast and wave optics conform solution. In: *Analyst* 143 (13), S. 3164–3175.

Photothermal Spectroscopy Corporation (2020): mIRage system manual. Hg. v. Photothermal Spectroscopy Corporation. Photothermal Spectroscopy Corporation. 325 Chapala St., Santa Barbara, CA 93101.

Attachment

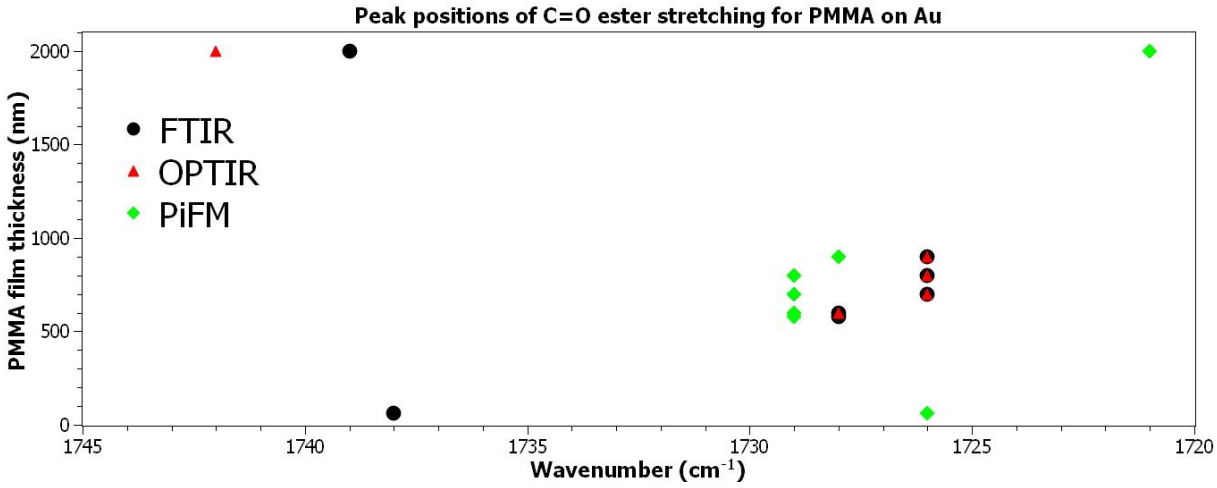

Figure A1: Shifting peak positions for various PMMA film thicknesses on Au of C=O ester stretching vibration for FTIR, O-PTIR and PiFM measurements.

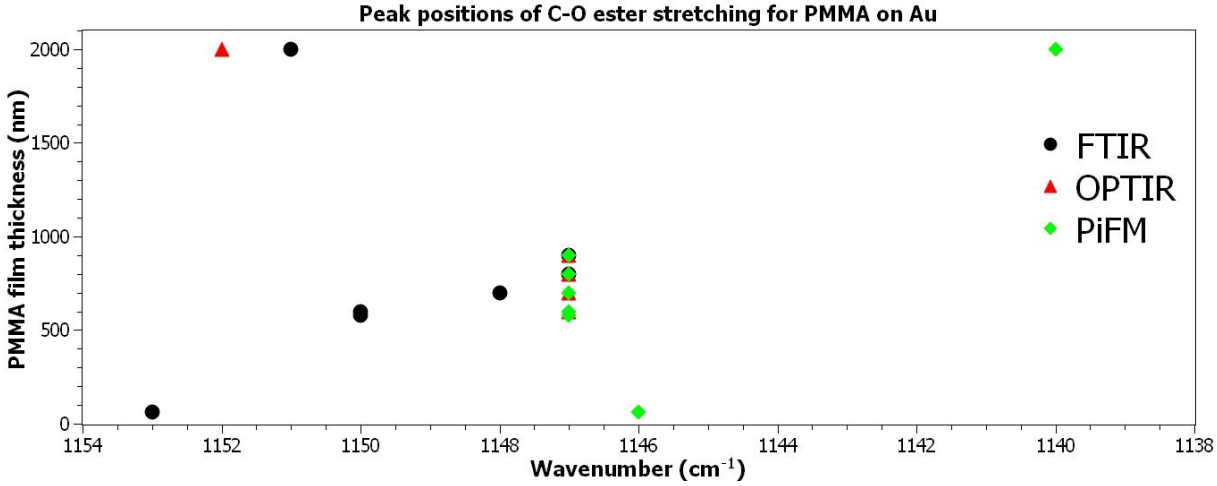

Figure A2: Shifting peak positions for various PMMA film thicknesses on Au of C-O ester stretching vibration for FTIR, O-PTIR and PiFM measurements.

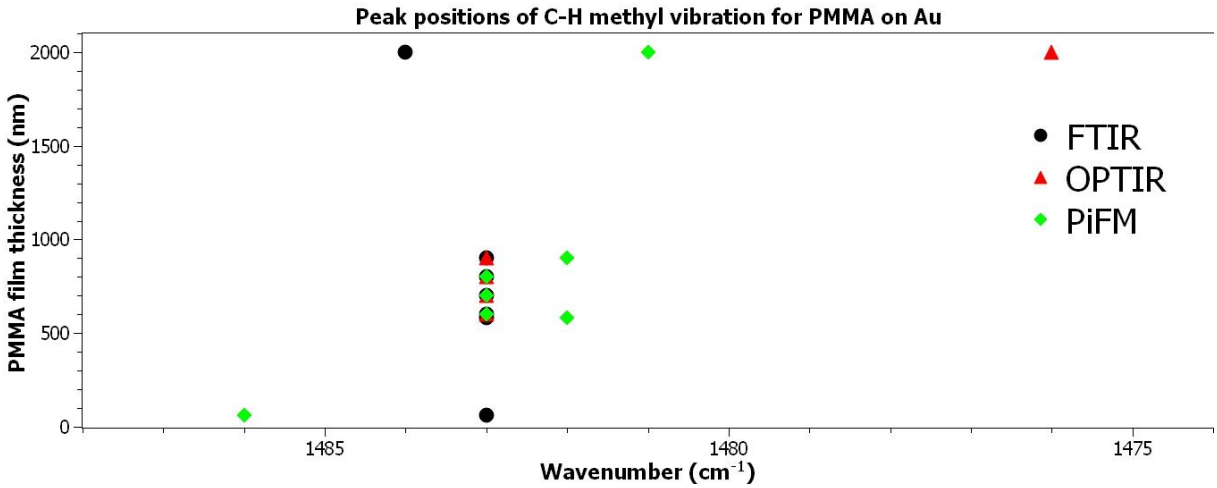

Figure A3: Shifting peak positions for various PMMA film thicknesses on Au of a C-H methyl bending vibration for FTIR, O-PTIR and PiFM measurements.